Clinical Anatomy 14:1–9 (2001)

ORIGINAL COMMUNICATIONS

Expanding the Boundaries of the Transsphenoidal Approach: A Microanatomic Study

ALBERTO ROMANO,[1] MARIO ZUCCARELLO,[2] HARRY R. VAN LOVEREN,[2] AND JEFFREY T. KELLER[2*]

[1]*University of Messina, Messina, Italy*
[2]*The Neuroscience Institute, Department of Neurosurgery, University of Cincinnati College of Medicine, Mayfield Clinic & Spine Institute, Cincinnati, Ohio*

The anatomic features of a transsphenoidal approach are reviewed, focusing on the microsurgical anatomy of parasellar structures. Pertinent microsurgical anatomy is described in sufficient detail for the neurosurgeon to successfully extend a standard transsphenoidal approach for treatment of lesions involving the region of the tuberculum sellae, planum sphenoidale, supradiaphragmatic intradural space, and medial cavernous sinus. The parasellar region of 50 formalin-fixed cadaveric heads was examined by using magnification 3× to 40×. The arterial and venous systems of five cadaveric specimens were injected under pressure with colored silicone rubber. The sellar region of three specimens was examined histologically. Important anatomic landmarks identified in the roof of the sphenoid sinus include a carotid and trigeminal prominence, as well as a tubercular, clival, and opticocarotid recess. The diaphragma sella is actually comprised of two layers of dura, with a venous system (circular sinus) interposed between the layers. The dura mater of the pituitary gland separates the gland from the medial compartment of the cavernous sinus. The microanatomic detail necessary to extend the transsphenoidal approach to the supradiaphragmatic intradural space and medial compartment of the cavernous sinus is described. These data are presented to facilitate the clinical application of these extended approaches. Clin. Anat. 14:1–9, 2001.

Key words: anatomy; cavernous sinus; supradiaphragmatic; transsphenoidal approach

INTRODUCTION

The microsurgical anatomy of the standard transsphenoidal approach has been well described by many investigators (Fujii et al., 1979; Ouaknine and Hardy, 1987a,b; Rhoton et al., 1979) and is familiar to most neurosurgeons. Although the transsphenoidal approach is the gold standard for the treatment of most pituitary tumors, complete surgical removal of lesions extending beyond the limit of the sella turcica remains problematic. Particularly challenging are lesions with a large supra- and/or parasellar extension that invades the hypothalamus and/or cavernous sinus, respectively.

Modifications of the transsphenoidal approach have been proposed in an attempt to enhance the surgical resection of these tumors (Fraioli et al., 1995; Lalwani et al., 1992; Mason et al., 1997; Petruson et al., 1997; Saito et al., 1995). Mason et al. (1997) recently described a surgical technique that extends the transsphenoidal approach to the planum sphenoidale, entering the suprasellar cistern to remove lesions at the level of the pituitary stalk. Fraioli et al. (1995) extended the transsphenoidal approach to the maxillary sinus to remove pituitary tumors invading the medial compartment of the cavernous sinus. These extensions of the transsphenoidal approach expose anatomic structures not frequently visualized during standard transsphenoidal surgery.

In this report, we provide a detailed description of the microsurgical anatomy of the structures that-

*Correspondence to: Jeffrey T. Keller, PhD, c/o Editorial Office, Department of Neurosurgery, University of Cincinnati College of Medicine, 231 Bethesda Avenue, Cincinnati, OH 45267-0515.

Received 30 August 1999; Revised 28 January 2000

surround the sella turcica, as seen from a transsphenoidal approach. Attention is focused on the specific anatomic details necessary to extend the transsphenoidal approach to the medial compartment of the cavernous sinus and the supradiaphragmatic intradural space.

MATERIALS AND METHODS

The sphenoid sinus region of the sella and suprasellar space was studied in 50 formalin-fixed human cadaveric heads. In five specimens, the arterial and venous systems were injected under pressure with colored silicone rubber (Dow Corning, Midland, MI, USA) via the internal carotid arteries and internal jugular veins, respectively. Microanatomical dissections were performed under magnification (3× to 40×), using a Contraves Zeiss Microscope (Carl Zeiss, Zeiss Company, Ober Kochen, Germany). Measurements were obtained by using calipers (Aesculap, Tuttlinger, Germany) and rulers in 36 cadaveric specimens.

The sellar region was harvested en bloc from three cadaveric specimens and prepared for histologic study. Specimens were placed in neutral buffered formalin 10% for 2 weeks, decalcified in Decalcifier I and II (Surgipath, Richmond, IL, USA) for 4 weeks, and then dehydrated, processed in a Citadel 2000 (Shandon, Pittsburgh, PA, USA) processor, and embedded in paraffin. Coronal or sagittal plane 6-μm sections were obtained by using a Reichert-Jung 2055 microtome (Cambridge Instruments, Heidelberg, Germany), heated at 65°C for 98 hr, and stained either in hematoxylin and eosin, or in Gomori's one-step Trichrome with Aniline Blue (Polyscientific, Bay Shore, NY, USA).

RESULTS

Sphenoid Sinus

The sphenoid sinus is generally divided in the sagittal plane by a bony septum that is frequently not midline. The sphenoid sinus can have multiple septi or no septum with a large single cavity. A detailed description of all possible variations of the sphenoid sinus septations was presented by Renn and Rhoton (1975). Depending on the extension of pneumatization, the sphenoid sinuses are classified by Hamberger et al. (1961) into three types: sellar type (86%), presellar type (11%), and conchal type (3%) (Fig. 1). The presellar and conchal types are more frequent in children and young adults because of the late development of the sphenoid sinus (complete pneumatization occurs at about age 20 years).

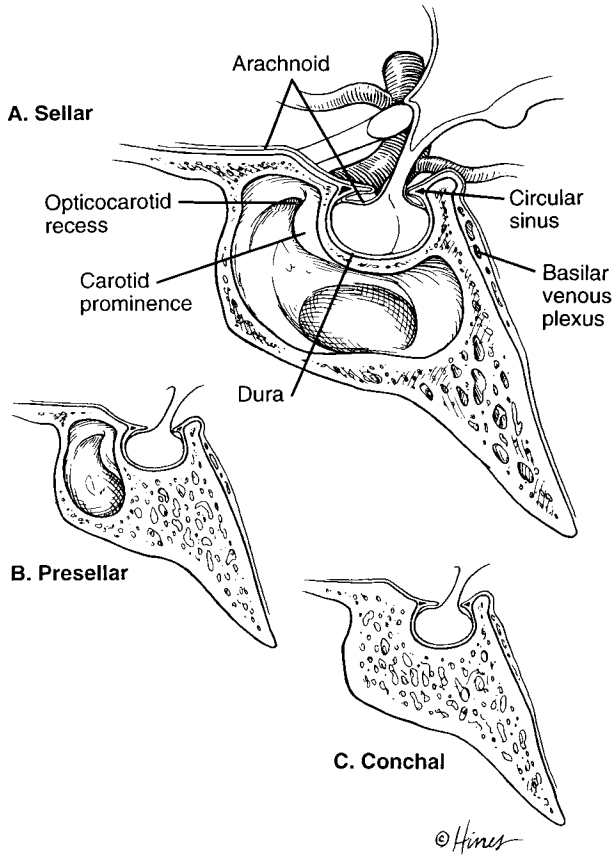

Fig. 1. Illustration of a midline sagittal view of the parasellar region and the three types of sphenoid sinuses: (A) sellar, (B) presellar, and (C) conchal. (Reprinted with permission from the Mayfield Clinic.)

The transsphenoidal view of the roof of the sphenoid sinus is shown in Figure 2. The sella turcica is seen as a prominence in the roof of a well-pneumatized sphenoid sinus. Lateral to the sella turcica, the carotid prominence is identified and corresponds to the cavernous segment (C4) and the clinoid segment (C5) of the internal carotid artery (ICA) (Bouthillier et al., 1996). The shape of the carotid prominence and the extent to which the prominence and the intracavernous ICA protrudes into the sphenoid sinus is quite variable. Occasionally, the entire length of the intracavernous ICA can be identified in the wall of sphenoid sinus. The bony wall of the carotid prominence is frequently less than 0.5 mm thick and occasionally dehiscent, making the artery extremely vulnerable. In the majority of cases, the bone of the carotid prominence is thinner than that forming the floor of the sella turcica. This thinness may lead the surgeon to mistakenly open the roof of the sphenoid sinus directly

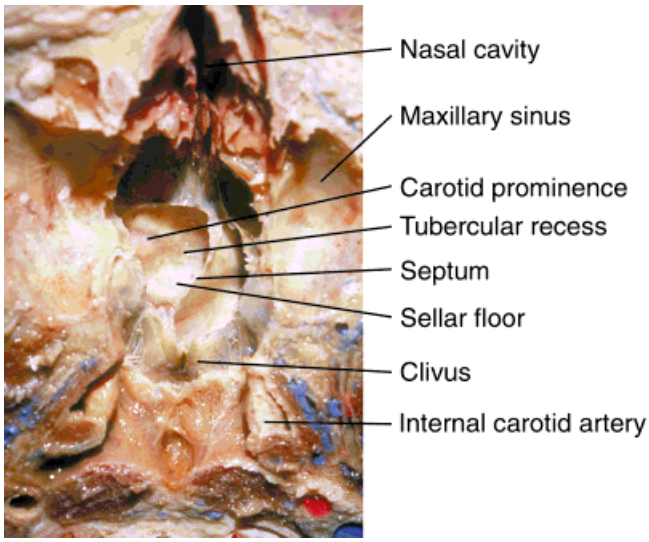

Fig. 2. Photograph of cadaveric dissection, axial section of skull base, inferior view, demonstrating the sphenoid sinus and adjacent structures. The septum of the sinus is deviated to the left. Structures identified include the sellar floor, carotid prominence with the C4 and C5 segments of the internal carotid artery, tubercular recess, internal carotid arteries, clivus, maxillary sinus, and nasal cavity. (Reprinted with permission from the Mayfield Clinic.)

over the ICA, in the belief that the floor of a sella, thinned by tumor, is being entered. The maxillary nerve (V2) courses along the inferolateral aspect of the wall of the sphenoid sinus, covered by bone that frequently protrudes into the sphenoid sinus, forming a trigeminal prominence (Fujii et al., 1979). Anterior and superior to the prominence produced by the sella turcica in the roof of the sphenoid sinus, there is a small recess that corresponds intracranially to the tuberculum sellae and chiasmatic sulcus. This recess is called the tubercular recess. However, the chiasmatic sulcus does not produce a prominence in the sphenoid sinus and, therefore, cannot be identified from the transsphenoidal view. The optic canals traverse the most anterior portion of the roof of the sphenoid sinus. Similar to the ICA, the bone that covers the optic nerves can be extremely thin or absent. The small recess located between the optic canal and the carotid prominence has been named the optico-carotid recess (Fujii et al., 1979). The optico-carotid recess corresponds to the junction between the optic strut and the body of sphenoid bone.

Posterior to the sella turcica, the roof of a well-pneumatized sphenoid sinus (sellar type) presents another recess whose posterior wall is the upper clivus. This region, when it exists, has been described endoscopically by Jho and Carrau (1996) as the clival indentation and is described here as the clival recess. The posterior wall of the sphenoid sinus corresponds to that segment of the clivus above the sphenooccipital synchondrosis (synostosis in adults). Depending on the degree of pneumatization of the sphenoid sinus, the thickness of the bone of the clival bone in this region varies considerably, ranging from 0.2 to 10 mm (mean 2.7) (Fujii et al., 1979). However, the posterior (clival) wall of the sphenoid sinus remains the thickest wall of the sphenoid sinus. The dura at this level is composed of two distinct layers (periosteum and dura propria). A very rich vascular plexus, the basilar sinus (rostral extension of Batson's venous plexus), which communicates with the cavernous sinus, is always present between these dural layers (Fig. 3). Bridging veins can be identified from the basilar sinus to the clival bone. The surgical working distance from the floor of the sphenoid sinus to the clival dura is a mean of 23.1 mm ($n = 6$) (range 18.9–25.5).

All the bony landmarks described inside the sphenoid sinus are evident in a well-pneumatized sphenoid sinus. However, it must be reemphasized that frequently, especially in younger patients, the bone of the sphenoid sinus walls may be thicker and some or all of the landmarks described may be obscured.

Dural Layers of the Sella Turcica and Medial Wall of Cavernous Sinus

After opening the floor of the sella turcica (Fig. 3), the dura mater covering the pituitary gland is identified. At this level, there are two distinct layers of dura.

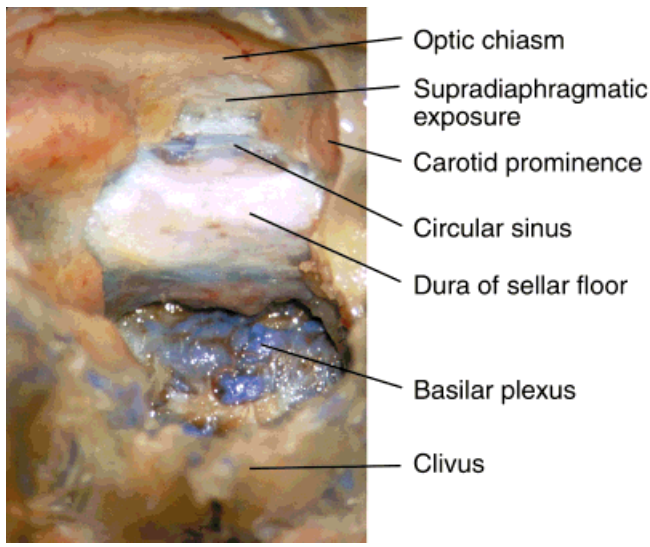

Fig. 3. Photograph of cadaveric dissection via a transsphenoidal approach. The floor of the sella and tuberculum sellae have been removed, exposing the dura of the sellar floor and the supradiaphragmatic region. Also identified are the optic chiasm and the carotid prominence. (Reprinted with permission from the Mayfield Clinic.)

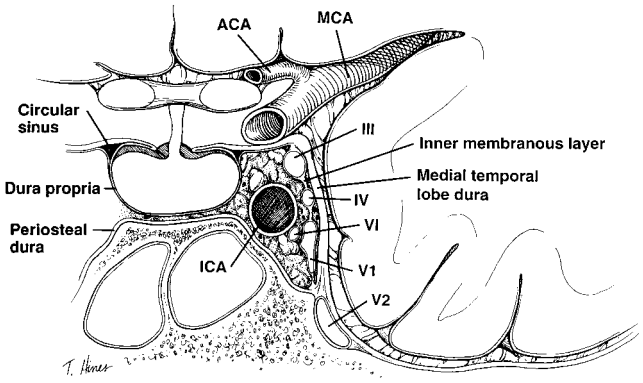

Fig. 4. Illustration of the coronal section showing the sellar and parasellar regions. Note the dural reflection of the diaphragma sella and its continuation laterally and inferiorly as the medial wall of the cavernous sinus. Cranial nerves III, IV, V_1, and V_2 of the lateral wall are seen within the inner membranous layer, whereas the internal carotid artery (ICA) and cranial nerve VI are intracavernous (ACA = anterior cerebral artery; MCA = middle cerebral artery). (Reprinted with permission from the Mayfield Clinic.)

One layer adjacent to the bone, the periosteal dura, covers the floor of the sella turcica, extends laterally beyond the sella, lines the carotid sulcus, where it forms part of the medial wall of cavernous sinus, and then continues as the floor of cavernous sinus. The dural layer adjacent to the pituitary gland separates the gland from the medial compartment of the cavernous sinus. Superiorly, this layer reflects to form the two layers of the diaphragma sella (Fig. 4). This reflection creates the central opening of the diaphragma sella through which the infundibulum passes. This layer continues laterally as the outer layer (dura propria) of the roof and lateral wall of cavernous sinus. Thus, the medial wall of the cavernous sinus has two separate components. In its upper aspect, the medial wall of the cavernous sinus is formed by the dural layer of the pituitary gland without bony support. In its lower aspect, the medial wall of the cavernous sinus is formed by the periosteal dura of the sella turcica and is supported by the bone of the lateral wall of the sphenoid sinus (Fig. 4). Our findings agree with the recent description by Destrieux et al. (1988) of the microanatomy of dural foldings in the sellar region. The mean distance between the two medial walls of the cavernous sinus was 14.9 mm (range 10.1–18.2) (n = 20). Renn and Rhoton (1975) reported the dimensions of the diaphragma sella as a mean width of 11 mm (range 5–13), and a mean length of 8 mm (range 5–13). The portion of diaphragma sella that is incised when the transsphenoidal approach is extended to the supradiaphragmatic intradural space, as described by Mason et al. (1997), is the portion between the central opening of the diaphragma sella and its insertion onto the tuberculum sellae. The mean length of this anterior portion is 3.3 mm (range 0–6.9) (n = 36). The central opening of the diaphragma sella has a mean width of 4.9 mm (range 2.1–10.3) (n = 36) and a mean length of 5.0 mm (range 2.0–10.3) (n = 36).

Venous channels commonly occupy the space between the two layers of dura in the sella turcica, and communicate between the two cavernous sinuses. Typically, these venous channels form both anterior and posterior intercavernous sinuses, which, in combination with the two cavernous sinuses, are called the circular sinus (Fig. 3). According to Renn and Rhoton (1975), the anterior intercavernous sinus is present in 76% of cases, and the posterior intercavernous sinus in 32% of the cases. Occasionally, these venous channels, and therefore the so-called circular sinus, can be found throughout the floor of the sella turcica.

Extension to the Supradiaphragmatic Intradural Space

The roof of the sphenoid sinus that is anterosuperior to the sella turcica is formed by the planum sphenoidale. The junction of the planum sphenoidale with the sella turcica forms a recess that we refer to as the tubercular recess (see section on Sphenoid Sinus). The bone of the tubercular recess and planum sphenoidale is frequently a thin layer of cortical bone. A small amount of cancellous bone can be found in the tuberculum sellae. The mean thickness of the bone of the tuberculum sellae is 1.0 mm (range 0.2–4.3), and that of the planum sphenoidale is 0.6 mm (range 0.2–1.4), as described by Fujii et al. (1979). The mean distance between the ICAs at the tuberculum sellae is 13.9 mm (range 10.0–17.0) (Fujii et al., 1979). The ICA at the level of the tuberculum sellae is relatively fixed by bone (anterior clinoid process, optic strut, and carotid sulcus of sphenoid bone) and by the distal dural ring. The relative immobility of the ICA at this level renders it more vulnerable to surgical injury during a transsphenoidal approach. The planum sphenoidale can be partially resected by transsphenoidal approach, but resection is limited laterally by the optic canals. The distance between the optic nerves at their entrance into the optic canal is 14 mm (range 9–24), according to Renn and Rhoton (1975).

The anterior intercavernous sinus, when present, demarcates the insertion of the diaphragma sellae into the tuberculum sellae (Fig. 5). The suprasellar cistern is exposed by dividing the anterior intercavernous sinus and diaphragma sellae and then opening the dura overlying the tuberculum sellae, chiasmatic sulcus, and pla-

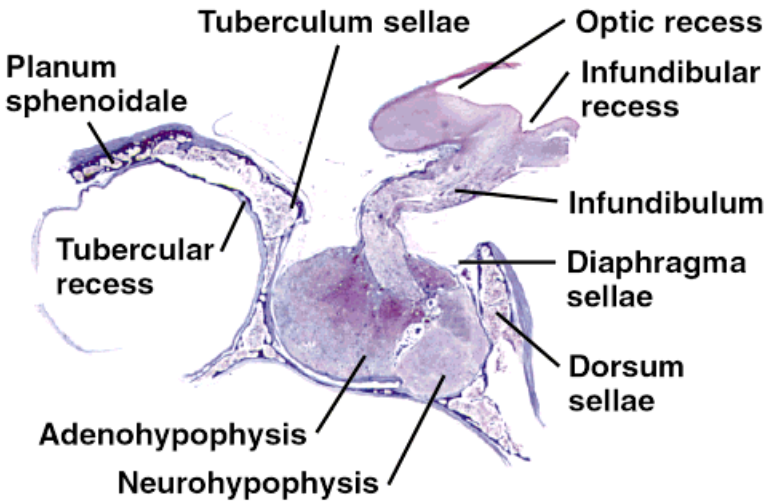

Fig. 5. Illustration of a histologic midline sagittal section (using Masson's trichrome stain, magnification 1×) of a human revealing the sella turcica and adjacent anterior and posterior bony structures, tuberculum sellae, and posterior clinoid process, respectively, as well as the planum sphenoidale. (Reprinted with permission from the Mayfield Clinic.)

num sphenoidale. Dissection of the arachnoid trabeculae then allows visualization of the pituitary stalk, optic chiasm, and superior hypophyseal arteries (Fig. 6). The superior hypophyseal arteries arise from the posteromedial surface of the ICA distally to the distal dural ring and vascularize the optic chiasm, pituitary stalk, and hypothalamus. Their number varies, ranging from one to four arteries on each side ($n = 35$) (mean 2.3 per side). Gibo et al. (1988) reported up to five superior hypophyseal arteries per side.

Medial Compartment of Cavernous Sinus

The medial compartment of the cavernous sinus is the portion of the cavernous sinus medial to the ICA (C4 segment) (Hakuba et al., 1989; Harris and Rhoton, 1976; Inoue et al., 1990). The dural component of the medial wall of the cavernous sinus has been described (see section on Dural Layers of the Sella Turcica and Medial Wall of Cavernous Sinus). No cranial nerves traverse the medial compartment. The ICA is, therefore, the first major structure encountered in exploration of the cavernous sinus in a transsphenoidal approach. The course of the ICA inside the cavernous sinus varies and has been described in detail by Harris and Rhoton (1976). In some cases, the carotid prominence is clearly visible and the entire course of the ICA can be identified prior to opening the sphenoid sinus wall. In other cases, portions of the

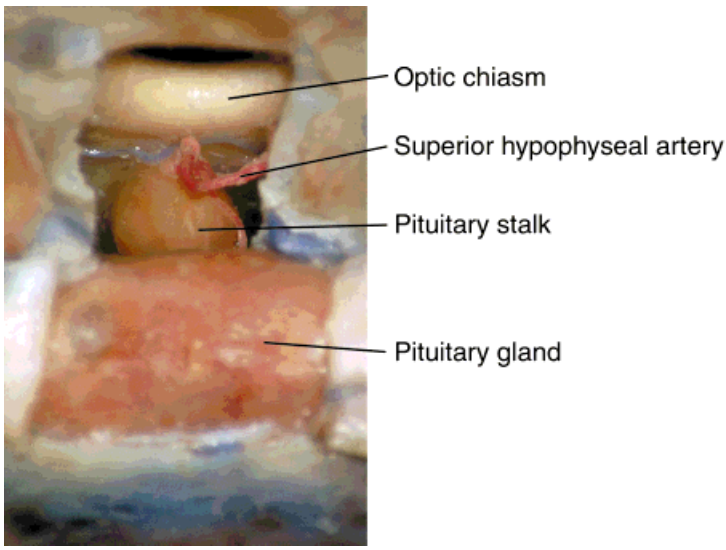

Fig. 6. Photograph of cadaveric dissection via a transsphenoidal approach illustrating the pituitary gland, pituitary stalk, superior hypophyseal artery, optic chiasm, and clivus. (Reprinted with permission from the Mayfield Clinic.)

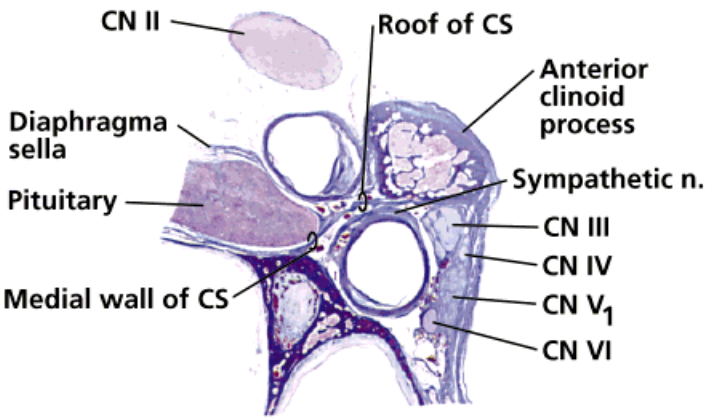

Fig. 7. Histologic coronal section of a human pituitary gland and adjacent right cavernous sinus (CS) showing the anterior clinoid process, two segments of the internal carotid artery, C4 and C6, and cranial nerves III–VI in the lateral wall of the CS. Note the dural reflections forming the diaphragma sella and the medial wall of the CS. (Reprinted with permission from the Mayfield Clinic.)

artery course far from the medial wall of the cavernous sinus and are separated from it by venous plexi. According to Fujii et al. (1979), the tuberculum sellae and the sellar floor are the points where the two carotid arteries come closer to the midline. In our specimens, the carotid artery frequently came in close contact with the pituitary gland, being separated only by the thin dura of the medial wall of the cavernous sinus (Fig. 7). The cavernous ICA is surrounded by a sympathetic plexus (Fig. 8). Cranial nerves III, IV, and VI of the cavernous sinus course through the lateral compartment and cannot be visualized in a transsphenoidal approach without mobilizing the ICA. The abducens nerve courses laterally and inferiorly to the cavernous ICA, and can sometimes be visualized from the medial compartment (Fig. 8).

DISCUSSION

The microsurgical transsphenoidal approach is the standard surgical treatment for most pituitary tumors and the microanatomic details of this approach are familiar to most neurosurgeons. However, extension of the transsphenoidal approach beyond the limits of the sella turcica into the cavernous sinus or the supradiaphragmatic intradural space remains a challenge. Modifications of the transsphenoidal approach to expose these areas have been described (Fraioli et al., 1995; Lalwani et al., 1992; Mason et al., 1997; Petruson et al., 1997; Saito et al., 1995). Because a thorough understanding of the extended microsurgical anatomy of the sphenoid sinus, sella turcica, and surrounding structures is critical to maintain the safety and efficacy of pituitary surgery, we discuss the microsurgical anatomy of the structures in the sellar region that are generally beyond the limits of a standard transsphenoidal approach (i.e., tuberculum sellae, planum sphenoidale, supradiaphragmatic intradural space, and medial cavernous sinus).

Suprasellar Extension

Suprasellar extension of pituitary tumors is relatively common. Saito et al. (1995) reported 100 (16%) cases of suprasellar extension in their series of 610 pituitary tumors. A standard transsphenoidal approach is commonly used to treat these lesions, supported by maneuvers that facilitate the descent of the tumor into the sella (e.g., Valsalva maneuver, jugular vein compression, and lumbar infusion). Other treatment options for a significant suprasellar extension of a tumor

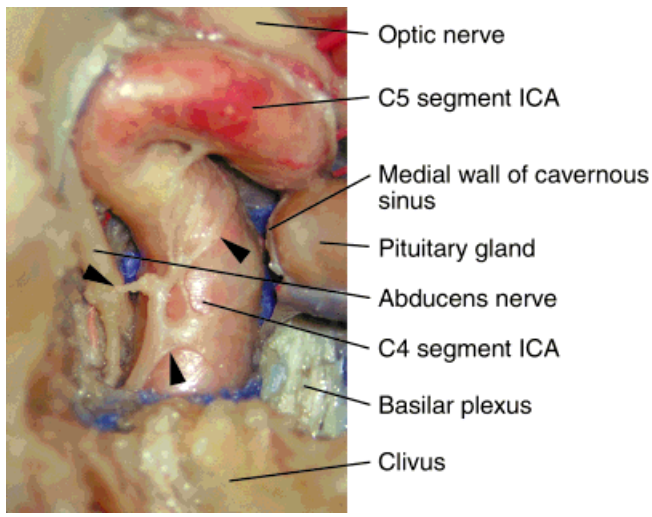

Fig. 8. Photograph of a cadaveric dissection using the transsphenoidal approach, illustrating the cavernous (C4) and clinoidal (C5) segments of the internal carotid artery (ICA). A prominent sympathetic plexus (arrowheads) is identified with a contribution to cranial nerve VI. The pituitary gland and medial wall of the cavernous sinus, optic nerve, clivus, and basilar plexus are also identified. (Reprinted with permission from the Mayfield Clinic.)

include staged transsphenoidal removal (Mohr et al., 1990; Saito et al., 1995), with or without the use of the open sella method (Saito et al., 1995), a combined transsphenoidal and intracranial approach (Burian et al., 1970; Laws et al., 1977; Loyo et al., 1984), and a transcranial approach only. Recently, Mason et al. (1997) described a transsphenoidal approach extended to the supradiaphragmatic intradural space to remove lesions at the level of the pituitary stalk. They utilized this approach for the treatment of four pituitary adenomas that were entirely supradiaphragmatic and six pituitary adenomas that extended from the sella to the supradiaphragmatic space.

The specific anatomic details required to accomplish supradiaphragmatic exposure are now examined beginning with description of the tubercular recess. The tubercular recess is a small recess of the sphenoid sinus anterior to the sella turcica, and corresponds intracranially to the tuberculum sellae and chiasmatic sulcus. The bone of the tubercular recess and planum sphenoidale is generally thin and can be resected by using rongeurs. The tuberculum sellae, however, can be thicker and require the use of a diamond burr. Lateral to the tubercular recess, is the ICA at the level of the distal dural ring. This is frequently the point at which the arteries come closest to one another (mean distance 13.9 mm) (Fujii et al., 1979). As previously stated, the ICA at this level is relatively fixed and, therefore, more vulnerable to surgical injury. Resection of the planum sphenoidale is limited laterally by the optic canal. The mean distance between the optic nerves at the entrance to the optic canals is 14 mm (Renn and Rhoton, 1975). Therefore, the bony window created by resection of the tuberculum sellae and planum sphenoidale that extends the transsphenoidal approach to the supradiaphragmatic intradural space, as described by Mason et al. (1997), is limited laterally by the ICA and optic canal to the extent of the dimensions given above. Division of the anterior intercavernous sinus (circular sinus) allows identification of the diaphragma sellae, which is then divided to its free edge at the central opening of the diaphragma sellae to expose the pituitary stalk. However, neither the presence nor the magnitude of the anterior intercavernous sinus is reliably predicted by magnetic resonance imaging/magnetic resonance venography. The mean length of this portion of the diaphragma sellae is 3.3 mm. This approach, which provides direct vision of the pituitary stalk and the inferior surface of the optic chiasm, facilitates resection of tumors that are confined to or extend into the supradiaphragmatic intradural space.

Prior to the report by Mason et al. (1997), Wilson type A pituitary adenomas that are dumbbell shaped with a suprasellar extension and a narrow waist at the diaphragma sellae were not thought to be resectable by transsphenoidal approach and required intracranial approach. The extended transsphenoidal approach of Mason et al. renders these pituitary adenomas amenable to transsphenoidal extirpation with acceptable results. However, neither the clinical nor the anatomical data should be misconstrued to imply that this approach should be applied to all pituitary tumors with large suprasellar extension (i.e., Wilson types B–D), because the safe resection of these adenomas is limited more by adherence to the optic chiasm, hypothalamus, and superior hypophyseal arteries than by lack of direct exposure.

Cavernous Sinus Invasion

An estimate of the percentage of pituitary tumors invading the cavernous sinus is difficult to ascertain from the literature. Magnetic resonance imaging cannot reveal a bulging of the medial wall of the cavernous sinus from a breach of the medial wall. Destrieux et al. (1998) found that a lateral expansion of the pituitary gland and its dural bag into the medial cavernous sinus was present in 29% of their specimens, speculating that an adenoma that developed in such an expansion could easily mimic cavernous sinus invasion. In our specimens, the pituitary gland frequently came in close contact with the ICA; occasionally the ICA looped medially, creating an impression on the pituitary gland, the "lateral expansion" described by Destrieux et al. (1998). Certainly encasement of the cavernous ICA defines cavernous sinus invasion. Selman et al. (1986) reported microscopic dural invasion in 85% of the pituitary adenoma cases examined. This study indicated a greater tendency for dural invasion than previously suspected, but did not specifically address cavernous sinus invasion. Jefferson (1990) stated that cavernous sinus invasion was not necessarily a simple consequence of tumor bulk. The common observation of unilateral cavernous sinus invasion supports the hypothesis that the integrity of the medial cavernous sinus wall may also be a factor in determining cavernous sinus invasion. Fraioli et al. (1995) described extension of the transsphenoidal approach to the maxillary sinus to expose sellar tumors (ten pituitary adenomas, one craniopharyngioma) invading the medial compartment of cavernous sinus.

The medial compartment of the cavernous sinus is separated from the pituitary gland by a thin,

single layer of dura mater (Fig. 7). Tumors invading the medial compartment generally obliterate the venous channels and thereby diminish the venous bleeding encountered during surgical dissection. Total removal of tumor from the medial compartment generally results in venous bleeding when dissection exposes the interface between tumor and the residual veins of the cavernous sinus not obliterated by the tumor. This venous bleeding actually indicates complete tumor removal in that area of dissection and is controlled by application of hemostatic agents. The absence of cranial nerves in the medial compartment renders resection of tumor from this compartment relatively safe, as long as ICA injury can be avoided. Fraioli et al. (1995) speculated that total resection of pituitary tumors from the medial compartment of the cavernous sinus by mobilization of the cavernous (C4) segment of the ICA was possible, based on a single case experience. This maneuver increases the risk of carotid artery injury, as well as the potential for cranial nerves morbidity, without documentation that total removal can be achieved once an adenoma has encased the ICA and occupied the lateral compartment. Therefore, resection of the tumor can be carried on safely if the surgeon is aware of the position of the ICA. The abducens nerve courses laterally and inferiorly to the ICA. Although dissection of the cavernous sinus is not so extensive as to expose this nerve, its position must be kept in mind, because excessive packing to control cavernous sinus bleeding may lead to its compression.

Sphenoid Sinus Invasion

Pituitary tumors commonly expand the sella turcica into the sphenoid sinus air space and occasionally invade the posterior sphenoid sinus and/or clivus. This region is accessible by the conventional transsphenoidal approach. The long working distance to the dura of clivus, the narrow angle of vision, and the presence of the basilar sinus limit the exposure of this region. Additional exposure is gained by extension of the transsphenoidal approach into the maxillary or ethmoid sinuses, according to Lalwani et al. (1992), but is beyond the scope of this article.

CONCLUSIONS

The requisite microanatomic detail necessary to extend the transsphenoidal approach to the supradiaphragmatic intradural space and medial compartment of the cavernous sinus has been described. These anatomic parameters have been related to reports of the successful clinical application of these extended surgical approaches, primarily for pituitary adenomas.

REFERENCES

Bouthillier A, van Loveren HR, Keller JT. 1996. Segments of the internal carotid artery: a new classification. Neurosurgery 38:425–433.

Burian K, Pendl G, Salah S. 1970. The recurrence of pituitary adenoma after transfrontal, transsphenoidal or two stage combined operations. Wien Med Wochenschr 120: 833–838.

Destrieux C, Kakou MK, Velut S, Lefrancq T, Jan M. 1998. Microanatomy of the hypophyseal fossa boundaries. J Neurosurg 88:743–752.

Fraioli B, Esposito V, Santoro A, Iannetti G, Giuffrè R, Cantore G. 1995. Transmaxillosphenoidal approach to tumors invading the medial compartment of the cavernous sinus. J Neurosurg 82:63–69.

Fujii K, Chambers SM, Rhoton AL, Jr. 1979. Neurovascular relationships of the sphenoid sinus: a microsurgical study. J Neurosurg 50:31–39.

Gibo H, Kobayashi Sh, Kyoshima K, Hokama M. 1988. Microsurgical anatomy of the arteries of the pituitary stalk and gland as viewed from above. Acta Neurochir (Wien) 90:60–66.

Hakuba A, Tanaka K, Suzuki T, Nishimura S. 1989. A combined orbitozygomatic infratemporal epidural and subdural approach for lesions involving the entire cavernous sinus. J Neurosurg 71:699–704.

Hamberger CA, Hammer G, Norlen G, Sjogren B. 1961. Transantrosphenoidal hypophysectomy. Arch Otolaryngol 74:2–8.

Harris FS, Rhoton AL, Jr. 1976. Anatomy of the cavernous sinus: a microsurgical study. J Neurosurg 45:169–180.

Inoue T, Rhoton AL, Jr, Theele D, Barry ME. 1990. Surgical approaches to the cavernous sinus: a microsurgical study. Neurosurgery 26:903–932.

Jefferson G. 1990. Extrasellar extensions of pituitary adenomas. Proc R Soc Med 33:433–458.

Jho H-D, Carrau RL. 1996. Endoscopy assisted transsphenoidal surgery for pituitary adenoma. Technical note. Acta Neurochir (Wien) 138:1416–1425.

Lalwani AK, Kaplan MJ, Gutin PH. 1992. The transsphenoethmoid approach to the sphenoid sinus and clivus. Neurosurgery 31:1008–1014.

Laws ER, Jr., Trautmann JC, Hollenhorst RW, Jr. 1977.Transsphenoidal decompression of the optic nerve and chiasm. Visual results in 62 patients. J Neurosurg 46:717–722.

Loyo M, Kleriga E, Mateos H, de Leo R, Delgado A. 1984. Combined supra-infrasellar approach for large pituitary tumors. Neurosurgery 14:485–488.

Mason RB, Nieman LK, Doppman JL, Oldfield EH. 1997. Selective excision of adenomas originating in or extending into the pituitary stalk with preservation of pituitary function. J Neurosurg 87:343–351.

Mohr G, Hardy J, Comtois R, Beauregard H. 1990. Surgical management of giant pituitary adenomas. Can J Neurol Sci 17:62–66.

Ouaknine GE, Hardy J. 1987a. Microsurgical anatomy of the pituitary gland and the sellar region. 1. The pituitary gland. Am Surg 53:285–290.

Ouaknine GE, Hardy J. 1987b. Microsurgical anatomy of the pituitary gland and the sellar region. 2. The bony structures. Am Surg 53:291–297.

Petruson K, Jakobsson KE, Petruson B, Lindstedt G, Bengtsson BA. 1997. Transsphenoidal adenomectomy in Cushing's disease via a lateral rhinotomy approach. Surg Neurol 48:37–45.

Renn WH, Rhoton AL, Jr. 1975. Microsurgical anatomy of the sellar region. J Neurosurg 43:288–298.

Rhoton AL, Jr, Hardy DG, Chambers SM. 1979. Microsurgical anatomy and dissection of the sphenoid bone, cavernous sinus and sellar region. Surg Neurol 12:63–104.

Saito K, Kuwayama A, Yamamoto N, Sugita K. 1995. The transsphenoidal removal of nonfunctioning pituitary adenomas with suprasellar extensions: the open sella method and intentionally staged operation. Neurosurgery 36:668–676.

Selman WR, Laws ER, Jr, Scheithauer BW, Carpenter SM. 1986. The occurrence of dural invasion in pituitary adenomas. J Neurosurg 64:402–407.